NeuroImage xxx (2015) xxx–xxx

Contents lists available at ScienceDirect

NeuroImage

journal homepage: www.elsevier.com/locate/ynimg

Functional connectivity hubs of the mouse brain

Adam Liska [a,b], Alberto Galbusera [a], Adam J. Schwarz [c], Alessandro Gozzi [a,*]

[a] Istituto Italiano di Tecnologia, Center for Neuroscience and Cognitive Systems @ UniTn, 38068 Rovereto, TN, Italy
[b] Center for Mind/Brain Sciences, University of Trento, Rovereto, TN, Italy
[c] Department of Psychological and Brain Sciences, Indiana University, Bloomington, IN, USA

ARTICLE INFO

Article history:
Received 28 December 2014
Accepted 16 April 2015
Available online xxxx

Keywords:
fMRI
Functional connectivity
Hubs
Mouse
Default mode network
Resting state

ABSTRACT

Recent advances in functional connectivity methods have made it possible to identify brain hubs — a set of highly connected regions serving as integrators of distributed neuronal activity. The integrative role of hub nodes makes these areas points of high vulnerability to dysfunction in brain disorders, and abnormal hub connectivity profiles have been described for several neuropsychiatric disorders. The identification of analogous functional connectivity hubs in preclinical species like the mouse may provide critical insight into the elusive biological underpinnings of these connectional alterations. To spatially locate functional connectivity hubs in the mouse brain, here we applied a fully-weighted network analysis to map whole-brain intrinsic functional connectivity (i.e., the functional connectome) at a high-resolution voxel-scale. Analysis of a large resting-state functional magnetic resonance imaging (rsfMRI) dataset revealed the presence of six distinct functional modules related to known large-scale functional partitions of the brain, including a default-mode network (DMN). Consistent with human studies, highly-connected functional hubs were identified in several sub-regions of the DMN, including the anterior and posterior cingulate and prefrontal cortices, in the thalamus, and in small foci within well-known integrative cortical structures such as the insular and temporal association cortices. According to their integrative role, the identified hubs exhibited mutual preferential interconnections. These findings highlight the presence of evolutionarily-conserved, mutually-interconnected functional hubs in the mouse brain, and may guide future investigations of the biological foundations of aberrant rsfMRI hub connectivity associated with brain pathological states.

Introduction

Resting-state BOLD functional magnetic resonance imaging (rsfMRI) has been widely employed to investigate the intrinsic functional organization of the human brain (Bullmore and Sporns, 2009). Graph theory representations of rsfMRI networks, whereby brain connectivity is conceptualized as a set of nodes (neuronal elements) and edges (their interconnections), have demonstrated that the human brain has topological features recapitulating the defining characteristics of complex networks (Watts and Strogatz, 1998), including the presence of functionally specialised modules encompassing well-characterised neurofunctional systems (Fair et al., 2009; Meunier et al., 2009; Power et al., 2011). In order to account for the brain's ability to simultaneously coordinate multiple network systems and ensure efficient communication, the presence of functional hub nodes serving as integrators of distinct neuronal systems has been hypothesised. Numerous rsfMRI studies have indicated the presence of highly-connected cortical regions as putative functional hubs for the human brain, most of which appear to exhibit overlap with sub-regions of the default mode network (DMN) (Cole et al., 2010; Tomasi and Volkow, 2011; Zuo et al., 2012). Importantly, the integrative role of these hub regions renders them points of potential vulnerability to dysfunction in brain disorders. Consistent with this notion, aberrant rsfMRI connectivity profiles have been described for several hub regions in pathological conditions such as autism, schizophrenia and neurodegenerative disorders (Buckner et al., 2009; van den Heuvel and Sporns, 2013). However, fundamental issues related to the etiopathological and biological foundations of these alterations remain to be addressed. For one, the neurophysiological cellular underpinnings of functional hub derangement observed in neuropsychiatric disorders remain largely unknown. It is also unclear whether these alterations are patho-physiologically relevant, or just epiphenomenal to underlying brain disorders.

Functional hub identification in preclinical species like the mouse, where genetic, cellular and molecular underpinnings of several brain disorders can be reproduced in controlled conditions and manipulated with cellular specificity (Deisseroth, 2011), may offer new critical insight into the above-mentioned issues. Initial attempts to unravel the rodent's brain functional topology have been carried out in rats (D'Souza et al., 2014; Liang et al., 2011, 2012) and more recently in mice (Mechling et al., 2014; Stafford et al., 2014). By using independent-component analysis (ICA) decomposition of rsfMRI signals in awake rats, Liang et al. (2011) reported the presence of three large modules, covering cortical areas, prefrontal and limbic hippocampal regions and basal forebrain

* Corresponding author.
E-mail address: alessandro.gozzi@iit.it (A. Gozzi).

http://dx.doi.org/10.1016/j.neuroimage.2015.04.033
1053-8119/

structures, respectively. Using anatomically-defined labels, D'Souza et al. (2014) identified six communities in medetomidine sedates rats, including two purely cortical systems (i.e., frontal and somatosensory) together with four mixed communities involving hippocampal and perihippocampal cortices, basal ganglia, thalamic nuclei and pons. ICA-based decomposition has also been recently applied to mouse rsfMRI datasets acquired under isoflurane anaesthesia (Mechling et al., 2014), leading to the identification of a basal ganglia module plus four other composite communities which included complex combinations of cortical and subcortical systems. Two of the above studies also report attempts to identify inter-connecting hub regions. D'Souza et al. (2014) attributed a putative integrative function to the hippocampus, striatum plus all cortical subdivision, with the sole exception of visual, primary motor and parietal cortices. These latter regions are part of a set of eleven putative hub regions described by Mechling in the mouse brain (2014), which also included somatosensory, frontal as well as subcortical diencephalic structures and the striatum. Collectively, while these initial studies led to the identification of seemingly stable functional partitions, substantial heterogeneity exists in their anatomical composition, as well as in the location of integrative structures, a finding that may reflect discrepant experimental procedures (e.g., anaesthesia, preprocessing procedures) and is probably exacerbated by heterogeneity in the regional parcellation schemes (coarse ICA-based, or anatomical volumes) and network thresholding strategies employed. Moreover, none of the functional partitions described so far can be straightforwardly related to known distributed human networks (e.g., DMN), which is a limiting factor in the translation of preclinical research to human condition.

Employing rigorous control of motion and potential physiological confounds (Ferrari et al., 2012), we recently demonstrated the presence of robust distributed rsfMRI networks in the mouse brain (Zhan et al., 2014), including functional precursors of the human salience and default mode networks (Sforazzini et al., 2014a,b), an observation recently replicated by an independent group (Stafford et al., 2014). Our datasets offer the opportunity to spatially locate functional hubs in the mouse brain and relate them to known network systems of the human brain, which greatly enhances the translational value of this approach. To this purpose, here we applied a computationally unbiased, fully-weighted network analysis of rsfMRI connectivity at a voxel scale in a large cohort of adult mice. We show the presence of six large-scale functional partitions, and anatomically localise mutually inter-connected hubs in several sub-regions of the DMN as well as in several cortical association areas of the mouse brain. These bear a strong resemblance to findings in the human brain, suggesting the presence of evolutionarily conserved cortical regions serving as integrators of segregated brain systems in the mouse, and supporting the use of this species to investigate aberrant rsfMRI hub connectivity associated to brain pathological states.

Materials and methods

All in vivo studies were conducted in accordance with the Italian law (DL 116, 1992 Ministero della Sanità, Roma) and the recommendations in the Guide for the Care and Use of Laboratory Animals of the National Institutes of Health. Animal research protocols were also reviewed and consented to by the animal care committee of the Istituto Italiano di Tecnologia (permit 07-2012). All surgical procedures were performed under anaesthesia.

Animal preparation

MRI experiments were performed on male 20–24 week old C57BL/6J (B6) mice (n = 41, Charles River, Como, Italy). The animal preparation protocol was recently described in detail (Ferrari et al., 2012; Sforazzini et al., 2014a,b; Zhan et al., 2014). Briefly, mice were anaesthetised with isoflurane (5% induction), intubated and artificially ventilated (2% maintenance). The left femoral artery was cannulated for continuous blood pressure monitoring and blood sampling. At the end of surgery, isoflurane was discontinued and substituted with halothane (0.75%). Functional data acquisition commenced 45 min after isoflurane cessation. Mean arterial blood pressure was recorded throughout the imaging sessions. Arterial blood gases (p_aCO_2 and p_aO_2) were measured at the end of the functional time series to exclude non-physiological conditions. Mean p_aCO_2 and p_aO_2 levels recorded were 20 ± 5 and 257 ± 33 mm Hg, respectively, well within the physiological range.

Image data acquisition

All in vivo experiments were performed using a 7.0 T MRI scanner (Bruker Biospin, Milan). Transmission and reception were achieved using a 72 mm birdcage transmit coil and a custom-built saddle-shaped four-channel solenoid coil for signal reception. Shimming was performed on a 6 mm × 6 mm × 6 mm region, using a FASTMAP protocol. For each session, high-resolution anatomical images were acquired with a fast spin echo sequence (RARE, Hennig et al., 1986) with the following parameters: repetition time (TR)/echo time (TE) 5500/60 ms, matrix 192 × 192, field of view 2 × 2 cm^2, 24 coronal slices, and slice thickness 0.50 mm. Co-centred single-shot BOLD rsfMRI time series were acquired using an echo planar imaging (EPI) sequence with the following parameters: TR/TE 1200/15 ms, flip angle 30°, matrix 100 × 100, field of view 2 × 2 cm^2, 24 coronal slices, slice thickness 0.50 mm, 300 volumes and a total rsfMRI acquisition time of 6 min.

Image data preprocessing

Image preprocessing was carried out using tools from FMRIB Software Library (FSL, v5.0.6; http://fsl.fmrib.ox.ac.uk/fsl/) (Jenkinson et al., 2012) and AFNI (v2011_12_21_1014; http://afni.nimh.nih.gov/afni/). RsfMRI time series were despiked (AFNI/3dDespike), corrected for motion (AFNI/3dvolreg), and spatially normalised to an in-house C57Bl/6J mouse brain template (Sforazzini et al., 2014b) (FSL/FLIRT, 12 degrees of freedom). The normalised data had a spatial resolution of 0.2 × 0.2 × 0.5 mm^3 (99 × 99 × 24 matrix). Head motion traces and mean ventricular signal (averaged fMRI time course within a manually-drawn ventricle mask) were regressed out of each of the time series (AFNI/3dDeconvolve). To assess the effect of global signal removal, separate rsfMRI time series with the whole-brain average time course regressed out were also generated. All rsfMRI time series were spatially smoothed (AFNI/3dmerge, Gaussian kernel of full width at half maximum of 0.5 mm) and band-pass filtered to a frequency window of 0.01–0.08 Hz (AFNI/3dBandpass) (Sforazzini et al., 2014b).

Functional network formation

Time courses from all voxels in a brain tissue mask associated with the anatomical template were extracted and a 16,135 × 16,135 connectivity matrix was calculated for each subject using Pearson product–moment correlation coefficient as a measure of inter-voxel connectivity (Bullmore and Sporns, 2009), resulting in subject-wise functional connectivity networks. In contrast to the vast majority of network analyses of rsfMRI data, the connectivity matrix was not subject to any further arbitrary thresholding and/or binarisation (Bullmore and Sporns, 2009). Separate connectivity matrices were created for the rsfMRI dataset with global signal regression.

Module detection

Most of network attributes used to identify functional hubs rely on a prior detection of modules that accurately describe the topological organization of brain networks (Sporns, 2013). To this purpose, standard approaches in human and rodent brain analyses employ a modular partition based on a connectivity network averaged across a large

Please cite this article as: Liska, A., et al., Functional connectivity hubs of the mouse brain, NeuroImage (2015), http://dx.doi.org/10.1016/j.neuroimage.2015.04.033

number of subjects (D'Souza et al., 2014; Liang et al., 2011, 2012; Mechling et al., 2014; Power et al., 2011, 2013; Rubinov and Sporns, 2010; Yeo et al., 2011; Zuo et al., 2012). Accordingly, the subject-wise connectivity matrices were first transformed to *z* scores using Fisher's *r*-to-*z* transform, averaged across all animals and transformed back to *r* values to create the average functional network.

The average functional network was then partitioned into non-overlapping modules by maximizing the modularity of the final partition (Newman and Girvan, 2004) using the Louvain algorithm (Blondel et al., 2008), as implemented in Brain Connectivity Toolbox (BCT) (Rubinov and Sporns, 2010). An asymmetric measure of modularity incorporating both positive and negative weights was employed (Rubinov and Sporns, 2011). Corresponding average null networks, against which we compared the resulting modularity value (Guimera et al., 2004), were created from subject-wise null networks, each matching the covariance structure of a single subject connectivity matrix (Zalesky et al., 2012).

The robustness of the resulting modules was further assessed by taking advantage of the non-deterministic nature of the Louvain algorithm (Blondel et al., 2008) and investigating the presence of competing maxima, whose presence is suggestive of an absence of a clear modular structure (Gfeller et al., 2005; Karrer et al., 2008; Massen and Doye, 2006; Wilkinson and Huberman, 2004). To this purpose, we performed 100 independent iterations of the algorithm, each with a randomized order of nodes on input, and created iteration stability maps of modules by calculating for each node the proportion of iterations in which it was assigned to each module. These iterations yielded a consistent output and, as further analyses required one single modular structure, a reference partition of the mouse functional network was created by assigning each voxel to the module to which it belonged in more than 50% of iterations. This procedure was carried out on rsfMRI datasets with and without global signal regression.

The two cortical modules identified in our study, the default mode network (DMN) and lateral cortical network (LCN), have been previously shown to be anticorrelated in both mice and rats (Schwarz et al., 2013a; Sforazzini et al., 2014b). To investigate the presence of analogous anticorrelations in the present dataset upon global signal regression, we extracted the mean signals from the identified cortical modules and correlated them with all voxels within the brain to obtain T statistics maps.

To assess inter-subject variability of the modular structure, subject-wise connectivity matrices were partitioned using the same method and the similarity of each pair of individual partitions was quantified with the variation of information (VI) metric (Rubinov and Sporns, 2011), achieving a mean VI value of 0.2412 (SD = 0.0203). The same procedure was repeated for subject-wise null networks, constructed as described above, achieving a mean VI value of 0.2889 (SD = 0.0116). A paired *t*-test between the corresponding VI values confirmed that the level of reproducibility is highly statistically significant ($p < 0.00001$). Moreover, the effect size obtained (2.9) was of similar order of magnitude to a recent rat study (D'Souza et al., 2014).

In order to assess the impact of spatial smoothing and voxel "adjacency" on the detection of functional modules (Power et al., 2011), we created two additional functional networks in which we removed connections shorter than 0.5 mm and 1.0 mm, respectively. We then separately identified modules in these two additional networks for comparisons with original functional partitions.

Global and module hub identification

Functional hubs have commonly been defined as nodes with a high density of connections across the whole network (Bullmore and Sporns, 2009). However, consideration of node connectivity distributions within and between the different component modules allows a more nuanced view of topological function and node roles within the overall network (Guimera and Amaral, 2005; van den Heuvel and Sporns, 2013; Zuo et al., 2012). In particular, it allows candidate hubs to be defined based on high connectivity within the overall network, within their own module and to nodes in other modules.

Normalised positive connection strength of a node in a weighted network (also referred to as strength) quantifies the overall density of its connections across the whole network and is defined as the sum of all positive connections of the node:

$$s_i \frac{\sum_{w_{ij}>0} w_{ij}}{N-1}$$

where w_{ij} is the weight of the connection between nodes *i* and *j*, and *N* is the number of nodes in the network (Rubinov and Sporns, 2011).

Conversely, connection diversity of a node assesses the distribution of its connections across modules, i.e., whether the node preferentially connects only to a limited subset of modules (low diversity) or whether its connections are spread evenly across the whole network (high diversity) (Rubinov and Sporns, 2011). The values of connection diversity are in the range of [0,1] and the measure is formally defined as:

$$h_i = -\frac{1}{\log M} s_i(u) \log s_i(u),$$

where *M* is the number of modules and $s_i(u)$ is the strength of node *i* within module *u*. The diversity parameter captures, for complete weighted networks, topological functionality analogous to the participation coefficient in binary networks (Guimera and Amaral, 2005).

The strength of node *i* within module *u* is defined as:

$$s_i(u) \frac{\sum_{w_{ij}>0} w_{ij}\delta_u(j)}{N-1},$$

where $\delta_u(j) = 1$ when *j* is part of module *u*, and $\delta_u(j) = 0$ otherwise (i.e., only connections of node *i* to nodes *j* within module *u* contribute to the summation) (Rubinov and Sporns, 2011). Within this framework, we refer to the strength of a node within its own module as the *within-module strength* of the node.

Guimera and Amaral (2005) elaborated a number of node roles in a "functional cartography" of the within- vs. between-module connectivity landscape of binary networks. While this presents an appealing conceptual framework, the proposed definitions were based on somewhat arbitrary (although intuitive) divisions of the parameter space. Analogous parameter-space divisions for fully weighted networks of functional connectivity have yet to be defined, and should meaningfully reflect both the network characteristics and underlying biology. A critical first step in elucidating the connectivity landscape of these neurobiological networks is to localise and understand the behaviour of the extreme nodes, i.e., those with maximal connection strength or diversity.

To identify and characterise extreme nodes, we implemented the statistical "top percentage" threshold approach (Cole et al., 2010), which identifies the highest strength and diversity regions and at the same time quantifies inter-subject consistency and avoids arbitrary strength or diversity thresholding. Briefly, this approach consists in calculating connection strength, connection diversity and within-module strength maps separately for each subject, converting them to standard scores and performing a series of one-tailed one-sample *t*-tests for each network attribute, comparing the value of the given attribute at each voxel to zero (its mean value). This results in a statistical map expressing the probability that the value of a given network attribute at a given voxel is higher than the average. A statistical threshold is then selected for each attribute such that only 10% of voxels remain. The reported threshold p-values were corrected using the false discovery rate (FDR) approach (Genovese et al., 2002); however, as it was already noted in Cole et al. (2010), this approach does not suffer from the multiple comparison problem as it does not rely on the use of statistical probabilities

Please cite this article as: Liska, A., et al., Functional connectivity hubs of the mouse brain, NeuroImage (2015), http://dx.doi.org/10.1016/j.neuroimage.2015.04.033

for threshold selection and FDR correction is applied in order to remain statistically conservative.

We identified as *global hubs* those nodes that exhibited high connection strength or connection diversity. Furthermore, we identified as *module hubs* those nodes that exhibited high within-module strength (Guimera and Amaral, 2005). To enable a direct comparison of our data with human and primate studies, where module and hub connectivity maps are typically reported for cortical areas, high connection diversity nodes in the two cortical modules were mapped separately.

In order to evaluate the reproducibility of the results with a smaller number of animals in an unbiased manner, 100 random subsets were created, each with exactly $N = 10$ animals. Hub regions were mapped independently for each group and we calculated the number of times out of 100 in which each voxel was identified as a hub of a given type. Furthermore, to assess the impact of higher temporal signal-to-noise ratio (tSNR) in cortical areas consequent to the use of surface coils (Kalthoff et al., 2011) on the network measure of connection strength, subject time series were corrupted with random pink noise throughout the brain such to achieve homogenous tSNR levels (≈ 25) equalling values observed in deep subcortical areas. Average tSNR values in representative regions of interest before pink noise corruption were as follows: 40.1 ± 3.5 in somatosensory cortex, 38.9 ± 2.9 in dorsal hippocampus, 35.7 ± 2.3 in cingulate cortex, 26.8 ± 1.8 in ventral thalamic areas, and 23.5 ± 2.0 in hypothalamus. After pink noise correction, tSNR values were 25.0 ± 1.1 in somatosensory cortex, 24.7 ± 0.4 in dorsal hippocampus, 24.8 ± 0.3 in cingulate cortex, 26.8 ± 1.5 in thalamus and 22.8 ± 0.8 in hypothalamus. The high strength global hub analysis was subsequently repeated for these time series after applying preprocessing steps described above.

Hub connectivity analysis

To assess whether the identified hubs are preferentially and mutually interlinked, we analysed their connectivity relationships using representative single-voxel seeds, each displaying the largest value of the network attribute in question for the given hub region (anatomical location in Fig. S1). We first mapped the strongest connections (thresholded at 90th percentile) of each candidate hub within each of the component modules. The presence of overlap between these hub 'seed maps' and module hub foci would suggest that the identified hubs exhibit reciprocal and preferential high strength connections, corroborating a role of these nodes as functional inter-module integrators.

The nature of the interconnected hub 'backbone' of the mouse functional connectome was then assessed directly by considering the network comprising only connections between the seeds. Mean hub–hub correlation values were extracted from the connection weights of the average functional network and the group-level significance of each connection was assessed using one-sample *t*-tests on *z*-transformed versions of the correlation coefficients. The tests were corrected for multiple comparisons using the Benjamini–Hochberg method and a false discovery rate of 0.01. A graph representation of the connections surviving statistical thresholding was displayed using the graph embedder (GEM) algorithm (Frick et al., 1995), as implemented in the Network Workbench package (http://nwb.cns.iu.edu/). The connectivity profile of each candidate hub was further assessed by computing the proportion of its connection strength into each module within the network.

Results

The mouse brain can be partitioned into six neurofunctional modules, including a default-mode cortical network

The network attributes used to identify functional hubs rely on a prior detection of modules that accurately describe the topological organization of brain networks. To map functional connectivity modules of the mouse brain at a high resolution and high degree of confidence, we computed the average inter-voxel rsfMRI connectivity in 41 male C57Bl/6J mice, and partitioned the resulting functional network into modules using a modularity-based algorithm (Blondel et al., 2008; Rubinov and Sporns, 2011). This approach led to the identification of five core cortical and sub-cortical functional modules, each manifesting a remarkably stable anatomical distribution across all repeated runs of the partitioning algorithm, and a single weaker module, composed of various thalamic nuclei, which appeared as an autonomous module in 60% of iterations and was split across neighbouring modules in the remaining iterations (Figs. 1A, B). The mean modularity of the functional network partitions (mean modularity $Q = 0.094729$, $\sigma = 0.000322$) was significantly higher than that of a corresponding null model (mean modularity $Q = 0.021335$, $\sigma = 0.000137$). Although we imposed no prior anatomical constraints, all six modules evidenced bilateral symmetry and strong correspondence with distributed functional and anatomical systems of the mammal brain. Specifically, the largest cortical module we identified extended along prefrontal midline structures to include bilateral posterior parietal and temporal association regions (Fig. 1A, Module 1). In the light of its remarkable similarity to the rodent precursor of the DMN (Lu et al., 2012; Schwarz et al., 2012, 2013b), a distributed cortical network recently described also in mice using seed-based correlations (Sforazzini et al., 2014b; Stafford et al., 2014), this module has been referred to as "DMN". A second cortical module, referred to as "lateral cortical network" (LCN), and including frontal association, anterior somatosensory, motor and insular cortices (Fig. 1A, Module 2), was identified. A similar network has been reliably identified in mice and rats using seed-based correlations (Schwarz et al., 2013a; Sforazzini et al., 2014b), and is topologically reminiscent of the human central executive network (Menon, 2011). The remaining three core modules consist mostly of well-characterised subcortical neuroanatomical systems of the mammal brain. The first of these modules encompassed dorsal and ventral hippocampal regions as well as a minor involvement of ventral retrosplenial areas (Fig. 1A, Module 3). A "basal forebrain" module was also apparent, including striatal and septal regions, the nucleus accumbens and anterior olfactory nucleus (Fig. 1A, Module 4). A fifth "ventral midbrain" module was identified to comprise several ventral brain regions including the amygdala, hypothalamus, and ventral tegmental area (Fig. 1A, Module 5). Finally, thalamic areas emerged as a clearly defined sixth module, although with lower inter-iteration stability (Fig. 1A, Module 6). Importantly, the partitioning of the functional network created from the same rsfMRI dataset upon global signal regression yielded consistent network modules (mean modularity $Q = 0.278539$, $\sigma = 0.001541$), with an increased stability of the thalamic module (Fig. S2), corroborating the robustness of the methodological approach and overall stability of the identified functional modules. Consistent with human data, the proportion of negative connections in the functional network upon global signal regression was increased from 13% to 52% (Murphy et al., 2009; Weissenbacher et al., 2009). Correlation analysis of the mean signals from the two cortical modules (DMN and LCN) in global signal regressed rsfMRI time series highlighted the presence of robust anticorrelations between these two modules (Fig. S3), thus providing additional empirical evidence of intrinsic anticorrelations between the two modules, a finding recently described in both mice and rats (Schwarz et al., 2013a; Sforazzini et al., 2014b).

To further confirm the robustness of our modular partition, and rule out bias from spatial smoothing and voxel adjacency artefacts (Power et al., 2013) we carried out a modular partition of functional network in which all connections shorter than 0.5 mm (approximately 2.5 voxels in plane) were removed, leading to the identification of a set of modules very consistent with those observed with full network (Fig. S4). With a much more stringent selection (i.e., removal of connections shorter than 1 mm, ca. 5 voxels in plane) modular instability was observed for subcortical modules, with evidence of stable partitioning of the DMN and thalamic modules as a single joint community (Fig. S4). This modular structure is consistent with previous seed-

Please cite this article as: Liska, A., et al., Functional connectivity hubs of the mouse brain, NeuroImage (2015), http://dx.doi.org/10.1016/j.neuroimage.2015.04.033

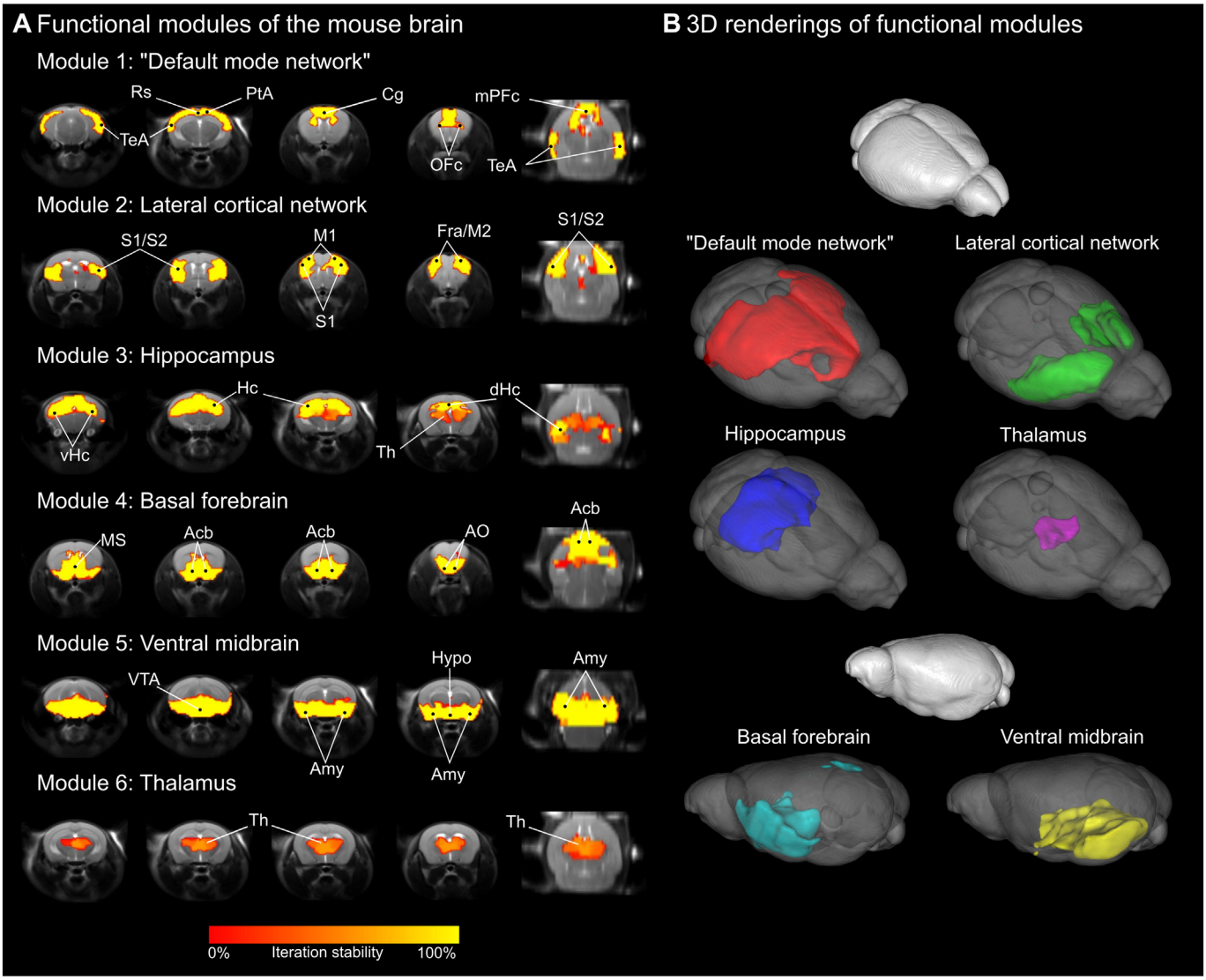

Fig. 1. Functional modules of the mouse brain. (A) Module stability maps (100 iterations, N = 41 subjects) overlaid on the anatomical template. For each module, four representative coronal slices (left) and one image in the horizontal plane (right) are shown. (B) Three-dimensional renderings of the reference partition within a transparent brain template. Opaque renderings show brain orientation. For a list of abbreviations, see Table 1.

based rsfMRI studies of the mouse brain, in which thalamic areas appear to be strongly correlated with cingulate and retrosplenial cingulate cortices (Sforazzini et al., 2014b). The appearance of subcortical modular instability upon removal of 1 mm connections is not unexpected, because 1 mm long connections cover the anatomical extension of some of the anatomical structures that constitute individual functional modules (e.g., radial hippocampus, or thalamus) (Paxinos and Franklin, 2004).

Global functional hubs are located in cingulate and prefrontal cortex

To identify functional hubs at a voxel scale, we first mapped connection strength values for all nodes in the functional network (Rubinov and Sporns, 2011). In agreement with human studies (Tomasi and Volkow, 2011), cortical and subcortical regions appeared to have distinct connectional profiles, with the former exhibiting much higher strength overall (Fig. 2A). Anatomical maps of the voxels exhibiting the highest strength ($p < 0.0001$, FDR corrected) revealed foci of high connection strength in several sub-regions of the DMN network, including the prefrontal, anterior and posterior cingulate cortex as well as parietal association regions (Fig. 2B).

To account for potential bias due to coil-induced regional variation in temporal signal to noise ratio (tSNR), we performed connection strength mapping on rsfMRI time series corrupted with random pink noise such to achieve homogenous tSNR levels equalling values observed in deep subcortical areas (≈25). The results of this analysis confirmed the original hub locations ($p < 0.0038$, FDR corrected, Fig. S5) thus ruling out a significant contribution of coil-related bias on high strength connection maps.

High connection diversity hubs are located in the thalamus and associative cortical areas

Connection diversity is a network attribute used to identify nodes participating in multiple functional sub-networks (Power et al., 2013; Rubinov and Sporns, 2011). Whole-brain mapping of nodes exhibiting high connection diversity ($p < 0.001$, FDR corrected) revealed a prominent involvement of thalamic areas (Figs. 2A, C), a finding consistent with the integrative and relay functions subserved by this region (Draganski et al., 2008).

To extrapolate and compare our results with human studies, where topological analyses are typically limited to cortical regions, we also generated a map of high connection diversity voxels within the identified neocortical modules (Figs. 3A, B). As recently described in humans (Power et al., 2011), nodes within the DMN module exhibited low

Please cite this article as: Liska, A., et al., Functional connectivity hubs of the mouse brain, NeuroImage (2015), http://dx.doi.org/10.1016/j.neuroimage.2015.04.033

Table 1
List of abbreviations.

Abbreviation	Description
Acb	Nucleus accumbens
Amy	Amygdala
AO	Anterior olfactory nucleus
AON	Anterior olfactory nucleus
BF	Basal forebrain module
CA1/3	CA1/3 fields of hippocampus
Cg	Cingulate cortex
CM	Central medial nucleus
dHc	Dorsal hippocampus
DMN	Default mode network
FrA	Frontal association cortex
Hc	Hippocampus/hippocampal module
Hypo	Hypothalamus
Ins	Insular cortex
LCN	Lateral cortical network
M1/2	Primary/secondary motor cortex
M2	Secondary motor cortex
mPFc	Medial prefrontal cortex
MS	Medial septal nucleus
OFc	Orbitofrontal cortex
P	Pons
PtA	Parietal association cortex
Rs	Retrosplenial cortex
S1/2	Primary/secondary somatosensory cortex
TeA	Temporal association cortex
Thal	Thalamus module
Th	Thalamus
vHc	Ventral hippocampus
VM	Ventral midbrain module
vSub	Ventral subiculum
VTA	Ventral tegmental area

average connection diversity, suggesting an extensive internal integration of this module and its function as a highly efficient "processing" system. Importantly, the approach also led to the identification of spatially restricted foci of high connection diversity in the temporal association cortex ($p < 0.001$, FDR corrected), a cortical area serving prominent integrative roles. Consistent with recent human studies (Power et al., 2013), foci of high connection diversity were also found in the anterior insular cortex ($p < 0.032$, uncorrected), although in this region the effect appeared to be less robust and did not survive FDR correction ($p < 0.2905$, FDR corrected).

Intra-module mapping of high connection hubs

To further investigate the topological organization of the individual sub-networks, we mapped, for each of the identified modules, voxels characterised by high within-module connectivity strength, which we refer to as "module hubs" (Figs. 4A, B). The top 10% voxels were statistically highly significant for all the modules, with the exception of the ventral midbrain module, where the FDR corrected p-value was, however, very close to significance level (DMN: $p < 0.000011$, LCN: $p < 0.00039$, Hc: $p < 0.0016$, basal forebrain: $p < 0.0068$, ventral midbrain: $p < 0.0572$, thalamus: $p < 0.0000096$, all FDR corrected). Module hub mapping in the default mode and lateral cortical networks highlighted high within-module strength foci in the anterior cingulate cortex, and frontal association cortices, respectively. Additional candidate module hubs were identified in the dorsal hippocampus (hippocampal module), nucleus accumbens and olfactory nuclei (basal ganglia), pons/ventral subiculum (ventral midbrain), and centromedial thalamic nuclei (thalamus).

Reproducibility of global and intra-module hub mapping on smaller subject cohorts

In order to evaluate the reproducibility of global and intra-module hub mapping on smaller subject cohorts, 100 random subject subsets each with exactly $N = 10$ animals were generated, and global and intra-module hub regions were mapped independently for each group. The results show robust conservation of most hub locations across the vast majority of randomly-generated 10-subject groups for global and module hubs (Fig. S6). Diversity hubs within the two cortical modules exhibited lower conservation, reflecting intrinsic lower stability and significance levels of these integrative locations as reported above.

The identified hubs are mutually and preferentially interconnected

To assess the presence of mutual inter-module connections between the identified hubs, the anatomical correspondence between the strongest connections of each source hub seed (Fig. S1) and the independently determined hub foci in other modules was investigated (Fig. 5). For the majority of the candidate hub pairs, the strongest connections of the source hub overlapped with voxels identified above as foci of maximal within module strength or connection diversity. This finding of robust and preferential hub–hub connections suggests that these brain regions act as a tightly interconnected sub-network within the mouse brain (Figs. 6A, C), underpinning cross-module integrative functions.

The interconnections between the eight candidate hubs were then characterised directly to better elucidate the module connectivity that they subserve (Fig. 6). Many, but not all, of the hub connections were significant, with the cingulate node (DMN module) having the highest number of significant connections (6) to other candidate hubs, and the temporal association cortex node (DMN) exhibiting the statistically

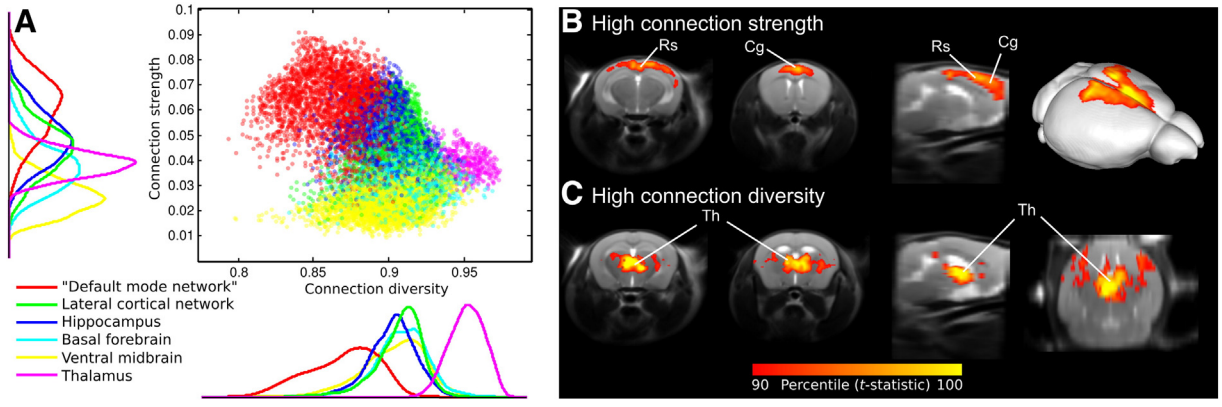

Fig. 2. Global hubs of the mouse brain. (A) Connection diversity and connection strength values are plotted for all nodes in the average functional network. Nodes are colour-coded according to their module. (B) Nodes surviving the top percentage threshold for connection strength are shown on two images in the coronal view (left), one image in the sagittal view (middle), and on a three-dimensional cortical surface rendering. (C) Nodes surviving the top percentage threshold for connection diversity are shown on two images in the coronal view, one image in the sagittal view (left), one image in the sagittal view (middle), and on a three-dimensional cortical surface rendering. For a list of abbreviations, see Table 1.

Please cite this article as: Liska, A., et al., Functional connectivity hubs of the mouse brain, NeuroImage (2015), http://dx.doi.org/10.1016/j.neuroimage.2015.04.033

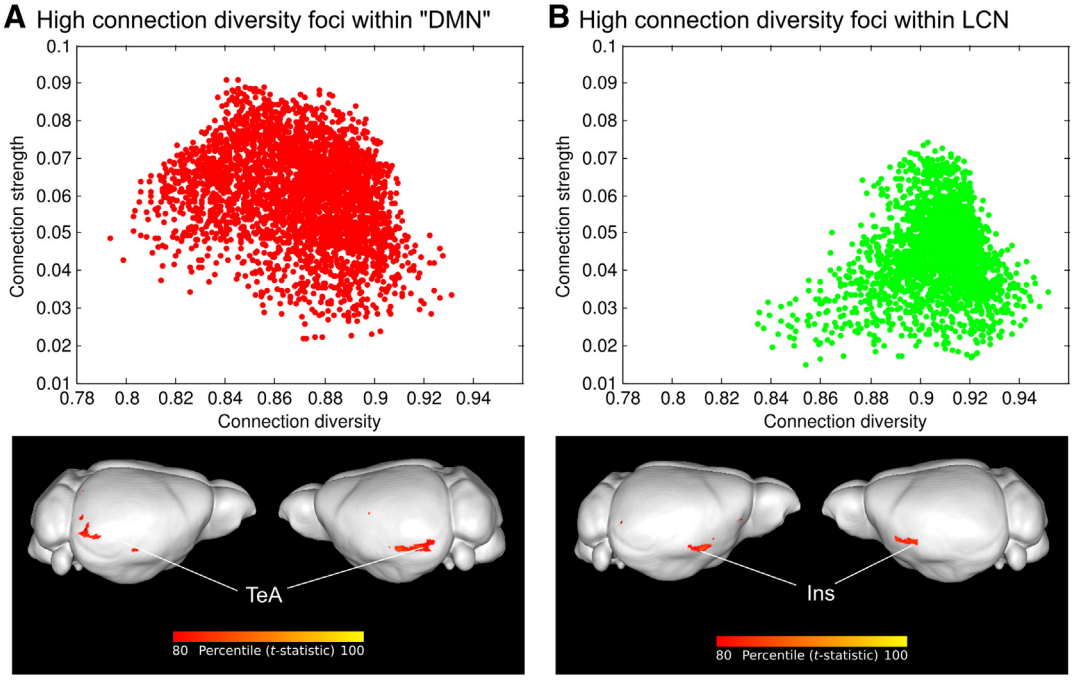

Fig. 3. High connection diversity regions within cortical modules. Connection diversity and strength values (calculated in the average functional network) are plotted for all nodes in the "default mode network" (A) and the lateral cortical network (B). Bottom panels highlight brain nodes surviving the top percentage threshold within each of the two cortical. The nodes are shown as three dimensional renderings on the cortical surface. For a list of abbreviations, see Table 1.

strongest connections, namely to the cingulate node (within-module) and to the frontal association cortex node (across-modules, LCN). The ventral subiculum node (VM module) had the least number (2) of significant connections to other candidate hubs, to the cingulate cortex and hippocampal nodes (both across-modules, DMN and Hc modules respectively). Notably, both the DMN and LCN modules each featured two putative cortical hubs, highlighting a key contribution of cortical hubs within these circuits (i.e., cingulate, temporal, frontal association, and insular cortices) as prominent integrative nodes of rsfMRI connectivity networks in the mouse brain.

The connectional profiles of candidate hubs attest to the widespread connectivity of hubs both within their own module and across the whole functional network (Fig. 6B). Interestingly, a prominent integrative role of the DMN module was apparent, as this region receives the largest share of the connection strength from all hubs (excepting connections within a hub's own module), although it is only second in size to the ventral midbrain module.

Discussion

We have demonstrated the presence of distinct functional modules in the mouse brain, and a set of anatomically localised, mutually interconnected candidate hub regions acting as cross-module functional integrators. Our approach provides a fine-grained description of the mouse functional connectome that can serve as a reference and complement ongoing research in the meso- and large-scale connectional

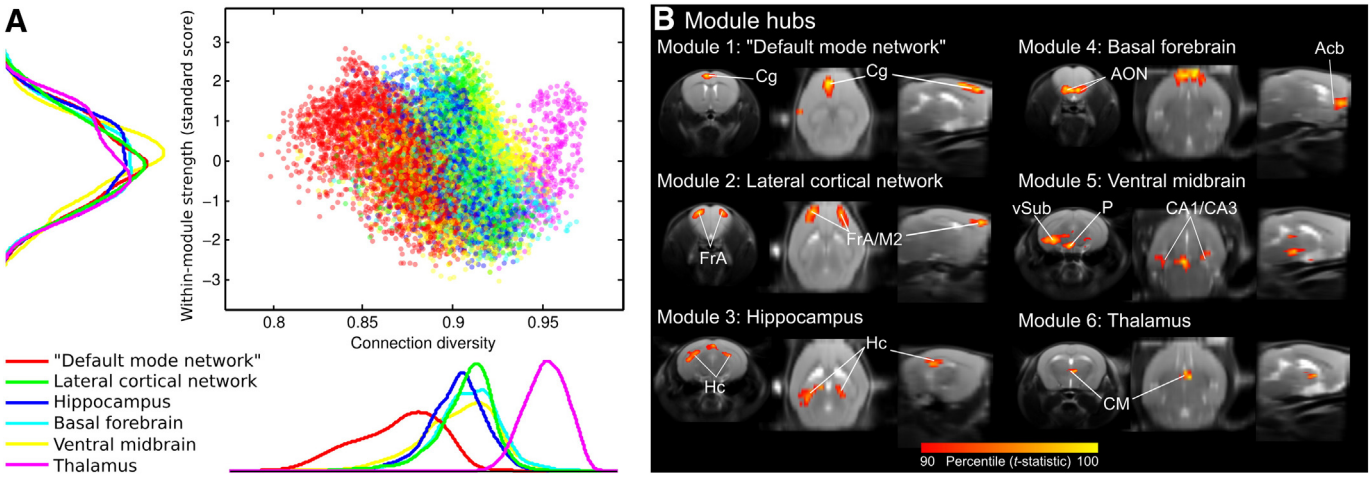

Fig. 4. Module hubs. (A) Connection diversity and normalised (z) scores of within-module strength plotted for all nodes in the average functional network. Nodes are colour-coded according to their module. (B) For each module, nodes surviving the top percentage threshold are shown on images in representative axial, horizontal and sagittal views of the mouse brain. For a list of abbreviations, see Table 1.

Please cite this article as: Liska, A., et al., Functional connectivity hubs of the mouse brain, NeuroImage (2015), http://dx.doi.org/10.1016/j.neuroimage.2015.04.033

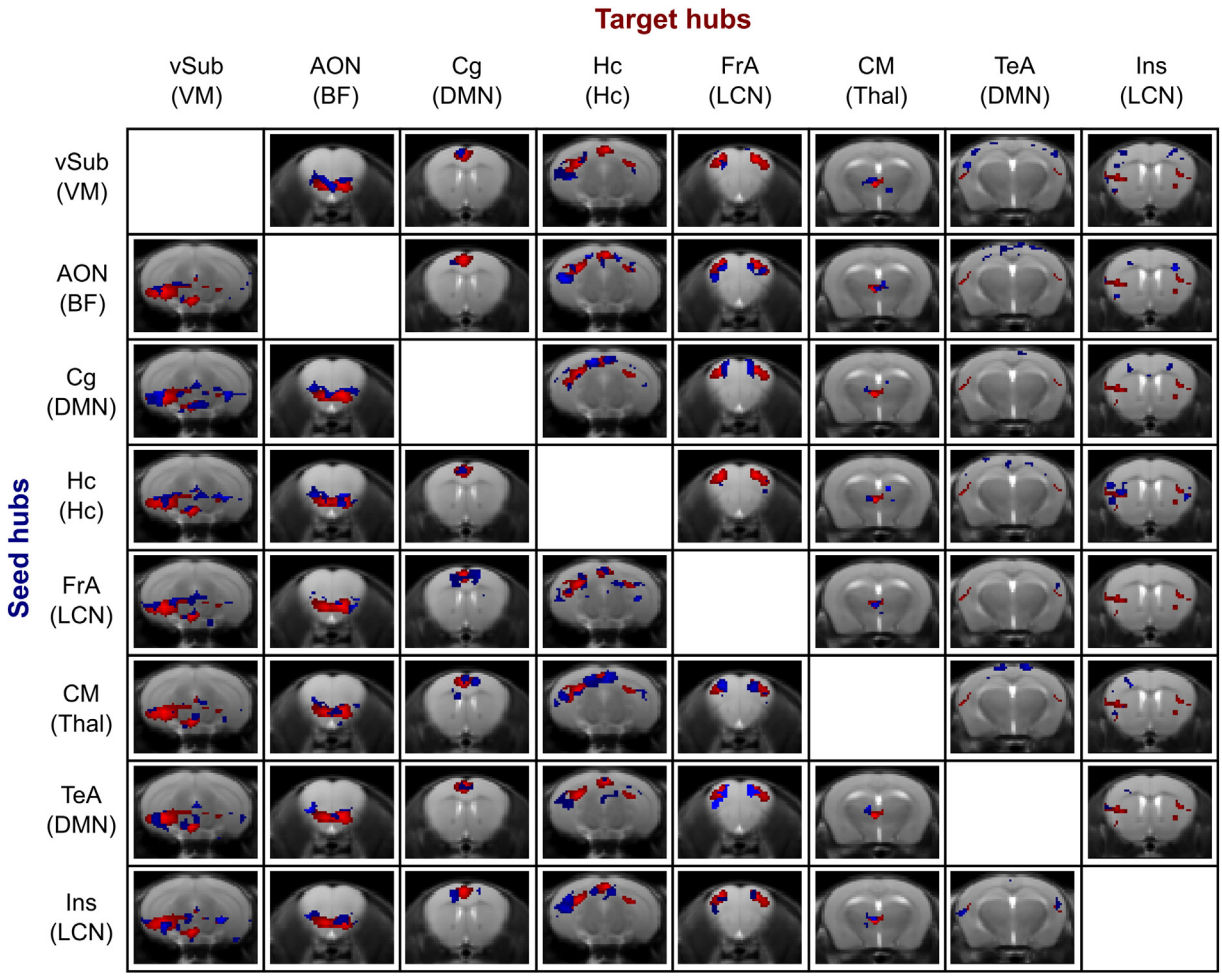

Fig. 5. Functional hubs are mutually interlinked. The strongest connections of each source hub to modules of target hubs (thresholded at 90th percentile for each module, in blue) are overlaid on top of target hub regions (in red). The results are shown on a representative coronal slice for each of the hub-module pair. For a list of abbreviations, see Table 1.

architecture of this species (Oh et al., 2014; Stafford et al., 2014; Zingg et al., 2014). It also opens the way to targeted manipulations of hub nodes in mouse models of brain pathology, a line of research that may advance our understanding of the elusive role of functional hub regions in neuropsychiatric states (van den Heuvel and Sporns, 2013). Importantly, we interrogated the mouse connectome at a high, voxel-scale spatial resolution and worked with fully-connected, fully-weighted networks, hence minimising bias induced by parcellation schemes and issues associated with arbitrary thresholding and/or binarisation (Bullmore and Sporns, 2009).

Modular organization is central to functional segregation in the brain, whereby distinct neuronal processing is performed by regions organized in functional modules (Sporns, 2013). Studies of functional modular organization in the human brain have consistently reported the presence of distinct distributed modules corresponding to known functional brain systems, such as the default mode, dorsal attention or somato-motor networks (Meunier et al., 2009; Power et al., 2011; Yeo et al., 2011). In keeping with this, the mouse brain functional networks identified here can be reliably related to established large-scale neuro-functional and neuroanatomical systems of the mammal brain. The detection of a DMN module using graph-based approaches is in good agreement with the results of classic (ICA- and seed-based) rsfMRI network mappings in the rodent brain (Schwarz et al., 2013a,b; Sforazzini et al., 2014b; Stafford et al., 2014) and underscores the pivotal role of this integrative network across mammal brain evolution (Lu et al., 2012). Similarly, the presence of a lateral cortical module is in agreement with recent seed-correlation and ICA rsfMRI studies in mice and rats where the presence of a similar DMN-anticorrelated system has been described (Schwarz et al., 2013a,b; Sforazzini et al., 2014b), thus leading to the hypothesis that such a network could be a precursor of lateralised "task-positive" executive modules present in humans and primates (Fox et al., 2005). Importantly, the identification of functionally-distinct antero-posterior distributed cortical module components is in excellent agreement with recent cortical connectivity mapping obtained with tracer injections in the mouse cortex. Indeed, by applying graph-based analyses of tracer-based structural connectivity, Zingg et al. (2014) identified two major neocortical clusters (i.e., somatic sensorimotor and medial antero-posterior networks) that exhibit remarkable neuroanatomical overlap with our LCN and DMN modules. Similarly, the same authors also identified two lateral integrative subnetworks in the cortex (anterior insular and posterior temporal) that can be related to the high connection diversity cortical hub nodes identified in the present work. Collectively, these findings corroborate the emerging view that functional correlations in spontaneous brain activity are constrained and guided by patterns of anatomical connectivity (Honey et al., 2009; Sui et al., 2014), a notion that has been more recently demonstrated also for the mouse brain (Stafford et al., 2014).

The correspondence between our cortical modules and analogous functional networks of the human brain is of high translational relevance, as the approach permits to identify key topological landmarks that can guide cross-species extrapolation of neural circuit research in health and pathology. In this respect, our work represents a significant advance over previous graph-based attempts to unravel the rodent's functional topology (Bifone et al., 2010; D'Souza et al., 2014; Liang et al., 2011, 2012; Schwarz et al., 2008, 2009). Indeed, while these

Please cite this article as: Liska, A., et al., Functional connectivity hubs of the mouse brain, NeuroImage (2015), http://dx.doi.org/10.1016/j.neuroimage.2015.04.033

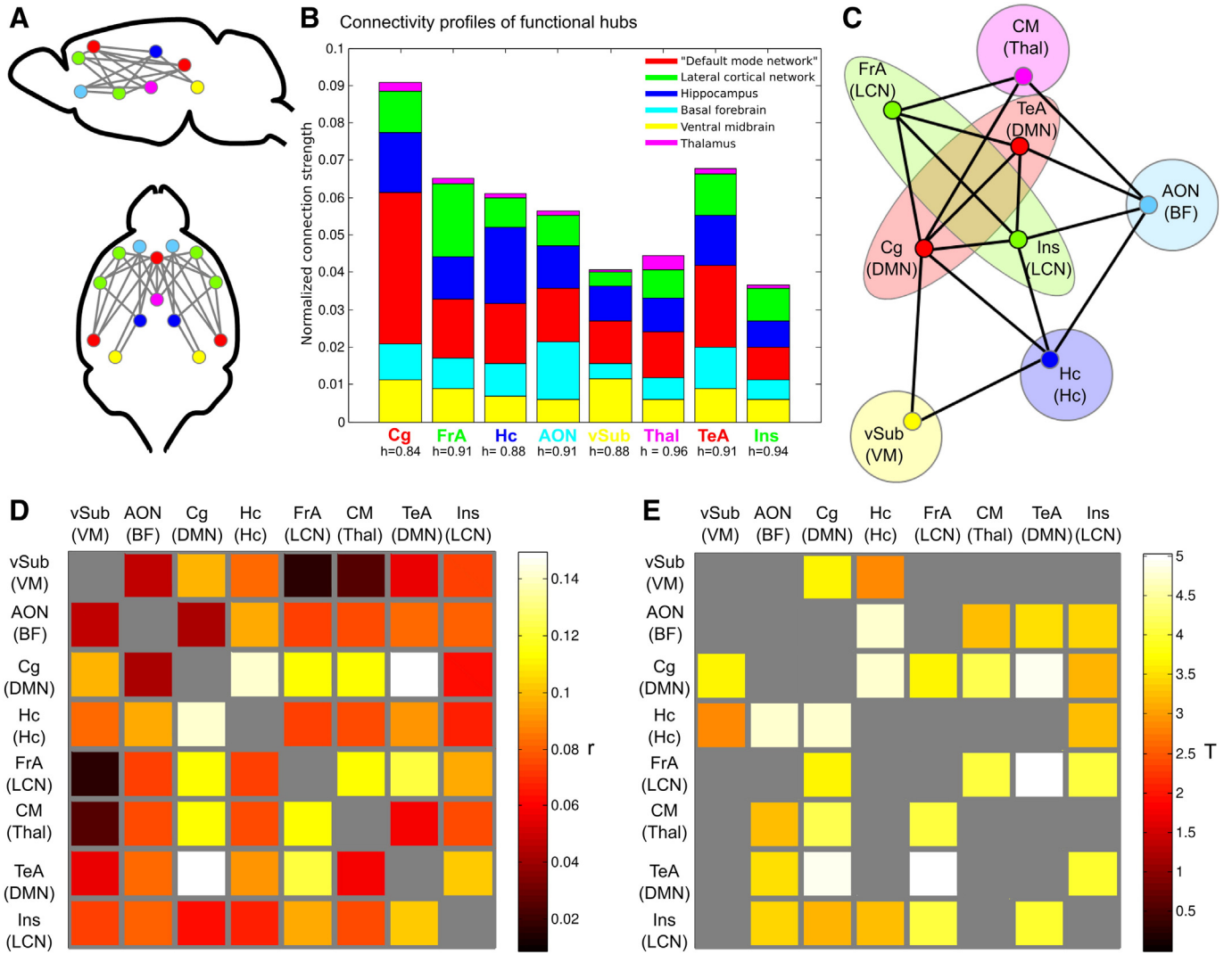

Fig. 6. Connectivity relationships of candidate hubs. (A) Approximate locations of candidate hubs of the mouse brain. Connections surviving statistical thresholding are indicated by a link between nodes (B) Connectivity profiles of candidate hubs, showing the proportion of their strength across all modules. (C) Graph representation of the connections surviving statistical thresholding, with node positions determined using the GEM algorithm. (D) Average correlation matrix for all pairs of identified hubs. (E) One sample *t*-tests for all pairs of identified hubs; non-significant connections (after FDR correction) are shown in grey. For a list of abbreviations, see Table 1.

previous studies identified plausible functional modules, including large cortical partitions (Liang et al., 2011) and some subcortical networks similar to those described here (e.g., basal ganglia and hippocampus) (D'Souza et al., 2014; Liang et al., 2011), they did not to reveal antero-posterior cortical networks like the rat's DMN module, or the lateral cortical system, a finding that could reflect discrepant experimental procedures as well as heterogeneity in the regional parcellation schemes (coarse ICA-based or anatomical volumes) and network thresholding strategies employed, or the fact that the initial graph-based parcellation used cross-subject analyses of responses to pharmacological stimuli (Bifone et al., 2010; Schwarz et al., 2008, 2009). Likewise, the results of a recent attempt to map functional modules and hubs in the mouse employing ICA-based functional parcellation (Mechling et al., 2014) resulted in a coarse modular organization that includes some of the modules identified in this study (e.g., basal ganglia and hippocampus), as well as a combination of cortical and subcortical structures encompassing multiple neurofunctional systems of the brain (e.g., sensory motor and limbic areas), which corroborate the underlying modular structure of the mouse brain, but cannot be directly related to analogous functional modules of the human brain. The identification of neuro-biologically interpretable functional modules is also key to the identification of candidate hub regions deemed to link and integrate specialised functional systems (Sporns, 2013). Using graph-based methods, numerous studies in humans have converged on a limited set of regions that occupy a central position in the functional topology of the human brain. These regions include anterior and posterior cingulate cortices, the insular cortex, and portions of superior frontal cortex, temporal cortex and lateral parietal cortex (Cole et al., 2010; Sporns, 2014; Tomasi and Volkow, 2011; van den Heuvel and Sporns, 2013). Importantly, the very same regions have also been shown to be implicated in the anatomy of various brain disorders, such as schizophrenia and Alzheimer's disease, which can be investigated and modelled in the mouse (Buckner et al., 2009; Crossley et al., 2014). Consistent with human findings (Cole et al., 2010), we identified high strength nodes in the mouse brain located in midline regions within the DMN module, with a predominant involvement of integrative areas such as the prefrontal, anterior and posterior cingulate cortex. Notably, a striking neuroanatomical correspondence also exists between our high connection strength hubs, and high degree structural connectivity hubs of the mouse brain based on axonal tracing (Stafford et al., 2014), a finding that recapitulates a fundamental neuro-architectural feature of the human brain (van den Heuvel and Sporns, 2013). Similarly, high connection diversity regions were identified in the temporal association cortex and, albeit with a lower degree of statistical confidence, also in

Please cite this article as: Liska, A., et al., Functional connectivity hubs of the mouse brain, NeuroImage (2015), http://dx.doi.org/10.1016/j.neuroimage.2015.04.033

the anterior insula, two areas classically implicated in multimodal integration (Gogolla et al., 2014). Furthermore, the same areas have been recently described in the human brain as regions of high participation coefficient, a binary network counterpart to connection diversity (Power et al., 2013). Importantly, most of the hub regions we identified in the mouse brain exhibit robust and specific mutual inter-connections, a finding which is consistent with an integrative functional role of these nodes, and which argues against a predominant confounding contribution of the correlational nature of rsfMRI-based networks (Power et al., 2013). Collectively, these correspondences underscore the translational relevance of our findings, and support the notion that the mouse brain contains evolutionary-conserved cortical foci serving as integrators of segregated systems in the mammal brain.

The fact that our experiments were performed in anaesthetised animals raises the question as to the degree to which the observed effects reflect the functional architecture of the mouse brain in conscious states. Two recent mouse rsfMRI studies have highlighted different connectivity signatures and reduced inter-hemispheric connectivity as a function of anaesthetic regimen (Grandjean et al., 2014; Jonckers et al., 2014). The present work was performed in halothane-anaesthetised animals, a regimen that appears to be particularly suited to map distributed rsfMRI circuits in this species for several reasons. First, halothane ensures motion control and stable hypnosis while preserving cerebral blood flow autoregulation (Gozzi et al., 2007) and cortical electrical responsiveness (Orth et al., 2006) without the occurrence of burst suppression activity, a phenomenon associated with significant rsFC alterations (Liu et al., 2011). Consistent with this, our recent work (Sforazzini et al., 2014a,b; Zhan et al., 2014) demonstrates the presence of (1) robust homotopic inter-hemispheric functional connectivity in both cortical and subcortical areas, and (2) distributed networks remarkably similar to those seen in conscious (and lightly anesthetised) rats and primates, anatomically homologous to the human salience network (SN) and default-mode network (DMN) (Hutchison et al., 2010; Lu et al., 2012; Rilling et al., 2007; Schwarz et al., 2012, 2013b; Vincent et al., 2007). Importantly, the observation of a DMN-like network in the mouse has been recently replicated by an independent group (Stafford et al., 2014) using a different anaesthetic (isoflurane), a finding that corroborates neurobiological foundations of this cortical module. Moreover, BOLD fMRI oscillations in the DMN-like network exhibit anti-correlations with neighbouring fronto-parietal areas, a cardinal feature of the human and primate DMN (Fox et al., 2005). By showing analogous networks using cerebral blood volume weighted signals, we also demonstrated that these spontaneous fluctuations are not significantly contaminated by large blood vessels (Sforazzini et al., 2014b). Finally, we recently demonstrated excellent spatial correspondence between rsfMRI signals obtained during light anaesthesia and electrophysiological coherence signals in freely-behaving animals, suggesting that the anaesthetic protocol negligibly influences intrinsic rsfMRI connectivity profiles (Zhan et al., 2014). Collectively, the identified rsfMRI networks exhibit significant correspondence with analogous measurements in awake habituated rats and human studies, thus legitimating the extrapolation of our results to conscious states. Consistent with this notion, global topological features of rsfMRI networks were found to be well maintained in the anaesthetised rat brain when compared to awake (restrained) states, despite the use of much higher (2.25-fold) minimal alveolar concentration levels of anaesthetic than the present work (Eger et al., 2003; Liang et al., 2012; Sonner et al., 2000). The remarkable overlap between modules and hubs identified in this work and recent tract tracing mapping in the mouse (Zingg et al., 2014), as well as analogous graph-based mappings in conscious human brain provide further empirical support to a marginal confounding contribution of anaesthesia to our findings.

Conclusions

In conclusion, our results describe topologically distinct neurofunctional modules of the mouse brain, including a DMN-like module, and identify a set of mutually-interconnected functional hubs that include well-characterised integrative cortical structures. These findings reveal the presence of evolutionarily conserved functional modules and integrative hubs in the mouse brain, and support the use of this species to investigate the elusive neurobiological underpinnings of the functional hub aberrations described for several pathological states. Importantly, our approach also provides a fine-grained description of the mouse functional connectome that complements and integrates ongoing research in the large-scale connectional architecture of this species.

Supplementary data to this article can be found online at http://dx.doi.org/10.1016/j.neuroimage.2015.04.033.

Acknowledgments

The authors are grateful to Stefano Panzeri and Angelo Bifone for critically reading the manuscript, and to Stefano Panzeri, for help with signal to noise simulation analyses. The study was funded by the Istituto Italiano di Tecnologia and by a grant from the Simons Foundation (SFARI 314688, A.G.).

Conflict of interests

The authors declare that they have no conflict of interest.

References

Bifone, A., Gozzi, A., Schwarz, A.J., 2010. Functional connectivity in the rat brain: a complex network approach. Magn. Reson. Imaging 28, 1200–1209.
Blondel, V.D., Guillaume, J.L., Lambiotte, R., Lefebvre, E., 2008. Fast unfolding of communities in large networks. J. Stat. Mech. Theory Exp. P10008 http://dx.doi.org/10.1088/1742-5468/2008/10/P10008.
Buckner, R.L., Sepulcre, J., Talukdar, T., Krienen, F.M., Liu, H.S., Hedden, T., Andrews-Hanna, J.R., Sperling, R.A., Johnson, K.A., 2009. Cortical hubs revealed by intrinsic functional connectivity: mapping, assessment of stability, and relation to Alzheimer's disease. J. Neurosci. 29, 1860–1873.
Bullmore, E., Sporns, O., 2009. Complex brain networks: graph theoretical analysis of structural and functional systems. Nat. Rev. Neurosci. 10, 186–198.
Cole, M.W., Pathak, S., Schneider, W., 2010. Identifying the brain's most globally connected regions. NeuroImage 49, 3132–3148.
Crossley, N.A., Mechelli, A., Scott, J., Carletti, F., Fox, P.T., McGuire, P., Bullmore, E.T., 2014. The hubs of the human connectome are generally implicated in the anatomy of brain disorders. Brain 137, 2382–2395.
Deisseroth, K., 2011. Optogenetics. Nat. Methods 8, 26–29.
Draganski, B., Kherif, F., Kloppel, S., Cook, P.A., Alexander, D.C., Parker, G.J., Deichmann, R., Ashburner, J., Frackowiak, R.S., 2008. Evidence for segregated and integrative connectivity patterns in the human basal ganglia. J. Neurosci. 28, 7143–7152.
D'Souza, D.V., Jonckers, E., Bruns, A., Kunnecke, B., von Kienlin, M., Van der Linden, A., Mueggler, T., Verhoye, M., 2014. Preserved modular network organization in the sedated rat brain. PLoS One 9, e106156.
Eger, E.I., Xing, Y.L., Laster, M., Sonner, J., Antognini, J.F., Carstens, E., 2003. Halothane and isoflurane have additive minimum alveolar concentration (MAC) effects in rats. Anesth. Analg. 96, 1350–1353.
Fair, D.A., Cohen, A.L., Power, J.D., Dosenbach, N.U., Church, J.A., Miezin, F.M., Schlaggar, B.L., Petersen, S.E., 2009. Functional brain networks develop from a "local to distributed" organization. PLoS Comput. Biol. 5, e1000381.
Ferrari, L., Turrini, G., Crestan, V., Bertani, S., Cristofori, P., Bifone, A., Gozzi, A., 2012. A robust experimental protocol for pharmacological fMRI in rats and mice. J. Neurosci. Methods 204, 9–18.
Fox, M.D., Snyder, A.Z., Vincent, J.L., Corbetta, M., Van Essen, D.C., Raichle, M.E., 2005. The human brain is intrinsically organized into dynamic, anticorrelated functional networks. Proc. Natl. Acad. Sci. U. S. A. 102, 9673–9678.
Frick, A., Ludwig, A., Mehldau, H., 1995. A fast adaptive layout algorithm for undirected graphs (extended abstract and system demonstration). In: Tamassia, R., Tollis, I. (Eds.), Graph Drawing. Springer Berlin Heidelberg, pp. 388–403.
Genovese, C.R., Lazar, N.A., Nichols, T., 2002. Thresholding of statistical maps in functional neuroimaging using the false discovery rate. NeuroImage 15, 870–878.
Gfeller, D., Chappelier, J.C., De Los Rios, P., 2005. Finding instabilities in the community structure of complex networks. Phys. Rev. E 72.
Gogolla, N., Takesian, A.E., Feng, G., Fagiolini, M., Hensch, T.K., 2014. Sensory integration in mouse insular cortex reflects GABA circuit maturation. Neuron 83, 894–905.
Gozzi, A., Ceolin, L., Schwarz, A., Reese, T., Bertani, S., Crestan, V., Bifone, A., 2007. A multimodality investigation of cerebral hemodynamics and autoregulation in pharmacological MRI. Magn. Reson. Imaging 25, 826–833.
Grandjean, J., Schroeter, A., Batata, I., Rudin, M., 2014. Optimization of anesthesia protocol for resting-state fMRI in mice based on differential effects of anesthetics on functional connectivity patterns. NeuroImage 102 (Pt 2), 838–847.

Guimera, R., Amaral, L.A.N., 2005. Cartography of complex networks: modules and universal roles. J. Stat. Mech. Theory Exp. P02001 http://dx.doi.org/10.1088/1742-5468/2005/02/P02001.

Guimera, R., Sales-Pardo, M., Amaral, L.A.N., 2004. Modularity from fluctuations in random graphs and complex networks. Phys. Rev. E 70.

Hennig, J., Nauerth, A., Friedburg, H., 1986. RARE imaging: a fast imaging method for clinical MR. Magn. Reson. Med. 3, 823–833.

Honey, C.J., Sporns, O., Cammoun, L., Gigandet, X., Thiran, J.P., Meuli, R., Hagmann, P., 2009. Predicting human resting-state functional connectivity from structural connectivity. Proc. Natl. Acad. Sci. U. S. A. 106, 2035–2040.

Hutchison, R.M., Mirsattari, S.M., Jones, C.K., Gati, J.S., Leung, L.S., 2010. Functional networks in the anesthetized rat brain revealed by independent component analysis of resting-state FMRI. J. Neurophysiol. 103, 3398–3406.

Jenkinson, M., Beckmann, C.F., Behrens, T.E., Woolrich, M.W., Smith, S.M., 2012. Fsl. NeuroImage 62, 782–790.

Jonckers, E., Delgado y Palacios, R., Shah, D., Guglielmetti, C., Verhoye, M., Van der Linden, A., 2014. Different anesthesia regimes modulate the functional connectivity outcome in mice. Magn. Reson. Med. 72, 1103–1112.

Kalthoff, D., Seehafer, J.U., Po, C., Wiedermann, D., Hoehn, M., 2011. Functional connectivity in the rat at 11.7 T: impact of physiological noise in resting state fMRI. NeuroImage 54, 2828–2839.

Karrer, B., Levina, E., Newman, M.E.J., 2008. Robustness of community structure in networks. Phys. Rev. E 77.

Liang, Z., King, J., Zhang, N., 2011. Uncovering intrinsic connectional architecture of functional networks in awake rat brain. J. Neurosci. 31, 3776–3783.

Liang, Z., King, J., Zhang, N., 2012. Intrinsic organization of the anesthetized brain. J. Neurosci. 32, 10183–10191.

Liu, X., Zhu, X.H., Zhang, Y., Chen, W., 2011. Neural origin of spontaneous hemodynamic fluctuations in rats under burst-suppression anesthesia condition. Cereb. Cortex 21, 374–384.

Lu, H.B., Zou, Q.H., Gu, H., Raichle, M.E., Stein, E.A., Yang, Y.H., 2012. Rat brains also have a default mode network. Proc. Natl. Acad. Sci. U. S. A. 109, 3979–3984.

Massen, C.P., Doye, J.P.K., 2006. Thermodynamics of Community Structure. eprint arXiv: cond-mat/0610077, p. 10077.

Mechling, A.E., Hubner, N.S., Lee, H.L., Hennig, J., von Elverfeldt, D., Harsan, L.A., 2014. Fine-grained mapping of mouse brain functional connectivity with resting-state fMRI. NeuroImage 96C, 203–215.

Menon, V., 2011. Large-scale brain networks and psychopathology: a unifying triple network model. Trends Cogn. Sci. 15, 483–506.

Meunier, D., Lambiotte, R., Fornito, A., Ersche, K.D., Bullmore, E.T., 2009. Hierarchical modularity in human brain functional networks. Front. Neuroinform. 3, 37.

Murphy, K., Birn, R.M., Handwerker, D.A., Jones, T.B., Bandettini, P.A., 2009. The impact of global signal regression on resting state correlations: are anti-correlated networks introduced? NeuroImage 44, 893–905.

Newman, M.E., Girvan, M., 2004. Finding and evaluating community structure in networks. Phys. Rev. E Stat. Nonlinear Soft Matter Phys. 69, 026113.

Oh, S.W., Harris, J.A., Ng, L., Winslow, B., Cain, N., Mihalas, S., Wang, Q., Lau, C., Kuan, L., Henry, A.M., Mortrud, M.T., Ouellette, B., Nguyen, T.N., Sorensen, S.A., Slaughterbeck, C.R., Wakeman, W., Li, Y., Feng, D., Ho, A., Nicholas, E., Hirokawa, K.E., Bohn, P., Joines, K.M., Peng, H., Hawrylycz, M.J., Phillips, J.W., Hohmann, J.G., Wohnoutka, P., Gerfen, C.R., Koch, C., Bernard, A., Dang, C., Jones, A.R., Zeng, H., 2014. A mesoscale connectome of the mouse brain. Nature 508, 207–214.

Orth, M., Bravo, E., Barter, L., Carstens, E., Antognini, J.F., 2006. The differential effects of halothane and isoflurane on electroencephalographic responses to electrical microstimulation of the reticular formation. Anesth. Analg. 102, 1709–1714.

Paxinos, G., Franklin, K.B., 2004. The Mouse Brain in Stereotaxic Coordinates. Gulf Professional Publishing.

Power, J.D., Cohen, A.L., Nelson, S.M., Wig, G.S., Barnes, K.A., Church, J.A., Vogel, A.C., Laumann, T.O., Miezin, F.M., Schlaggar, B.L., Petersen, S.E., 2011. Functional network organization of the human brain. Neuron 72, 665–678.

Power, J.D., Schlaggar, B.L., Lessov-Schlaggar, C.N., Petersen, S.E., 2013. Evidence for hubs in human functional brain networks. Neuron 79, 798–813.

Rilling, J.K., Barks, S.K., Parr, L.A., Preuss, T.M., Faber, T.L., Pagnoni, G., Bremner, J.D., Votaw, J.R., 2007. A comparison of resting-state brain activity in humans and chimpanzees. Proc. Natl. Acad. Sci. U. S. A. 104, 17146–17151.

Rubinov, M., Sporns, O., 2010. Complex network measures of brain connectivity: uses and interpretations. NeuroImage 52, 1059–1069.

Rubinov, M., Sporns, O., 2011. Weight-conserving characterization of complex functional brain networks. NeuroImage 56, 2068–2079.

Schwarz, A.J., Gozzi, A., Bifone, A., 2008. Community structure and modularity in networks of correlated brain activity. Magn. Reson. Imaging 26, 914–920.

Schwarz, A.J., Gozzi, A., Bifone, A., 2009. Community structure in networks of functional connectivity: resolving functional organization in the rat brain with pharmacological MRI. NeuroImage 47, 302–311.

Schwarz, A.J., Gozzi, A., Chessa, A., Bifone, A., 2012. Voxel scale complex networks of functional connectivity in the rat brain: neurochemical state dependence of global and local topological properties. Comput. Math. Methods Med. 2012, 615709.

Schwarz, A.J., Gass, N., Sartorius, A., Risterucci, C., Spedding, M., Schenker, E., Meyer-Lindenberg, A., Weber-Fahr, W., 2013a. Anti-correlated cortical networks of intrinsic connectivity in the rat brain. Brain Connect. 3, 503–511.

Schwarz, A.J., Gass, N., Sartorius, A., Zheng, L., Spedding, M., Schenker, E., Risterucci, C., Meyer-Lindenberg, A., Weber-Fahr, W., 2013b. The low-frequency blood oxygenation level-dependent functional connectivity signature of the hippocampal–prefrontal network in the rat brain. Neuroscience 228, 243–258.

Sforazzini, F., Schwarz, A.J., Galbusera, A., Bifone, A., Gozzi, A., 2014a. Distributed BOLD and CBV-weighted resting-state networks in the mouse brain. NeuroImage 87, 403–415.

Sforazzini, F., Bertero, A., Dodero, L., David, G., Galbusera, A., Scattoni, M.L., Pasqualetti, M., Gozzi, A., 2014b. Altered functional connectivity networks in acallosal and socially impaired BTBR mice. Brain Struct. Funct. http://dx.doi.org/10.1007/s00429-014-0948-9.

Sonner, J.M., Gong, D., Eger, E.I., 2000. Naturally occurring variability in anesthetic potency among inbred mouse strains. Anesth. Analg. 91, 720–726.

Sporns, O., 2013. Network attributes for segregation and integration in the human brain. Curr. Opin. Neurobiol. 23, 162–171.

Sporns, O., 2014. Towards network substrates of brain disorders. Brain 137, 2117–2118.

Stafford, J.M., Jarrett, B.R., Miranda-Dominguez, O., Mills, B.D., Cain, N., Mihalas, S., Lahvis, G.P., Lattal, K.M., Mitchell, S.H., David, S.V., Fryer, J.D., Nigg, J.T., Fair, D.A., 2014. Large-scale topology and the default mode network in the mouse connectome. Proc. Natl. Acad. Sci. U. S. A. 11 (52), 18745–18750.

Sui, J., Huster, R., Yu, Q., Segall, J.M., Calhoun, V.D., 2014. Function–structure associations of the brain: evidence from multimodal connectivity and covariance studies. NeuroImage 102P1, 11–23.

Tomasi, D., Volkow, N.D., 2011. Functional connectivity hubs in the human brain. NeuroImage 57, 908–917.

van den Heuvel, M.P., Sporns, O., 2013. Network hubs in the human brain. Trends Cogn. Sci. 17, 683–696.

Vincent, J.L., Patel, G.H., Fox, M.D., Snyder, A.Z., Baker, J.T., Van Essen, D.C., Zempel, J.M., Snyder, L.H., Corbetta, M., Raichle, M.E., 2007. Intrinsic functional architecture in the anaesthetized monkey brain. Nature 447, 83–86.

Watts, D.J., Strogatz, S.H., 1998. Collective dynamics of 'small-world' networks. Nature 393, 440–442.

Weissenbacher, A., Kasess, C., Gerstl, F., Lanzenberger, R., Moser, E., Windischberger, C., 2009. Correlations and anticorrelations in resting-state functional connectivity MRI: a quantitative comparison of preprocessing strategies. NeuroImage 47, 1408–1416.

Wilkinson, D.M., Huberman, B.A., 2004. A method for finding communities of related genes. Proc. Natl. Acad. Sci. U. S. A. 101, 5241–5248.

Yeo, B.T., Krienen, F.M., Sepulcre, J., Sabuncu, M.R., Lashkari, D., Hollinshead, M., Roffman, J.L., Smoller, J.W., Zollei, L., Polimeni, J.R., Fischl, B., Liu, H., Buckner, R.L., 2011. The organization of the human cerebral cortex estimated by intrinsic functional connectivity. J. Neurophysiol. 106, 1125–1165.

Zalesky, A., Fornito, A., Bullmore, E., 2012. On the use of correlation as a measure of network connectivity. NeuroImage 60, 2096–2106.

Zhan, Y., Paolicelli, R.C., Sforazzini, F., Weinhard, L., Bolasco, G., Pagani, F., Vyssotski, A.L., Bifone, A., Gozzi, A., Ragozzino, D., Gross, C.T., 2014. Deficient neuron–microglia signaling results in impaired functional brain connectivity and social behavior. Nat. Neurosci. 17.

Zingg, B., Hintiryan, H., Gou, L., Song, M.Y., Bay, M., Bienkowski, M.S., Foster, N.N., Yamashita, S., Bowman, I., Toga, A.W., Dong, H.W., 2014. Neural networks of the mouse neocortex. Cell 156, 1096–1111.

Zuo, X.N., Ehmke, R., Mennes, M., Imperati, D., Castellanos, F.X., Sporns, O., Milham, M.P., 2012. Network centrality in the human functional connectome. Cereb. Cortex 22, 1862–1875.

Please cite this article as: Liska, A., et al., Functional connectivity hubs of the mouse brain, NeuroImage (2015), http://dx.doi.org/10.1016/j.neuroimage.2015.04.033